ADVANCED FUNCTIONAL MATERIALS
www.afm-journal.de

www.MaterialsViews.com

Open-Circuit Voltage and Effective Gap of Organic Solar Cells

Johannes Widmer, Max Tietze, Karl Leo,* and Moritz Riede*

The open-circuit voltage (V_{OC}) of an organic solar cell is limited by the donor-acceptor material system. The effective gap E_g^{eff} between the electron affinity of the acceptor and the ionization potential of the donor is usually regarded as the upper limit for V_{OC}, which is only reached for $T \rightarrow 0$ K. This relation is confirmed for a number of small-molecule bulk heterojunction p-i-n type solar cells by varying the temperature and illumination intensity. With high precision, the low temperature limit of V_{OC} is identical to E_g^{eff}. Furthermore, the influence of the hole transport material in a p-doped hole transport layer and the donor-acceptor mixing ratio on this limit V_0 is found to be negligible. Varying the active material system, the quantitative relation between V_0 and E_g^{eff} is found to be identity. A comparison of V_0 in a series of nine different donor-acceptor material combinations opens a pathway to quantitatively determine the ionization potential of a donor material or the electron affinity of an acceptor material.

1. Introduction

Organic solar cells promise to be one of the major applications for organic semiconductors and are rapidly approaching commercial viability. Vacuum deposited small molecular organic semiconductors are an established technology in the field of organic light emitting diodes and will soon be available in organic photovoltaic products.[1] Recently, considerable progress in device efficiency has been achieved,[2] mainly by new and improved materials employed in the devices. In highly efficient devices, the absorbers are typically incorporated in a bulk heterojunction of the donor and acceptor material.[3,4] The design of organic solar cells made of small molecules by vacuum deposition can be tuned by control of the doped transport layers,[5] absorber layers, and other organic or inorganic layers.[6–8] The layers can be arranged with many degrees of freedom, including the realization and fine-tuning of tandem devices.[9–11] Beyond these possibilities for stack optimization, the efficiency is dominated by the photoactive heterojunction materials.[12,13] The photocurrent and the charge extraction throughout the device are depending on transport and extraction processes.[14–16]

The photovoltage, in contrast, depends on the energy of the electronic states upon exciton separation.[17,18] In p-i-n type solar cells, it is related to the effective energy gap of the donor-acceptor material combination used in the photoactive heterojunction, rather than the electrodes and their work function.[5,19] The effective gap, i.e. the difference between the electron affinity of the acceptor and the ionization potential of the donor, is regarded as the upper limit of the open-circuit voltage.[19] However, the quantitative correlation with the open-circuit voltage at room temperature is still a matter of debate.[20–23]

In this work, we experimentally confirm with high precision that the linear extrapolation of the open-circuit voltage in a p-i-n type solar cell to 0 K is a property of the donor-acceptor material system and equals the effective energy gap between donor and acceptor. Furthermore, we show that V_0 is not a function of a transport layer adjacent to the active layer, but is determined by the bulk heterojunction only. Furthermore, we demonstrate that calibration of our method with one well characterized material system allows for the determination of the ionization potential of a donor material or the electron affinity of an acceptor material. We emphasize here that the use of p-i-n cells with their well-defined built-in field and contacts is an important factor to obtain reproducible and stable data for open-circuit voltages.

2. Theoretical Methods

The open-circuit voltage V_{OC} of a solar cell originates from the difference between the quasi-Fermi levels in the electron and hole extracting regions of the device.[24,25] In organic solar cells based on a donor-acceptor bulk heterojunction, it ideally corresponds to the quasi-Fermi level splitting between electrons and holes within the bulk.[26] In the presence of well-conducting transport layers, the Fermi levels in the transport layers equal the respective quasi-Fermi levels in the bulk, if there are no injection barriers present.[16] According to an equivalent circuit model based on a diode and a current source modeling the photocurrent, V_{OC} is a function of both the photocurrent and temperature T. Typically the photocurrent of a solar cell – organic or inorganic – is proportional to the illumination intensity I. In this case V_{OC} can be expressed as

J. Widmer, M. Tietze, Prof. K. Leo, M. Riede[+]
Institut für Angewandte Photophysik (IAPP)
TU Dresden, 01062 Dresden, Germany
E-mail: johannes.widmer@iapp.de; leo@iapp.de
[+]Present address: Clarendon Laboratory
University of Oxford, Parks Road, Oxford OX1 3PU, England, UK

DOI: 10.1002/adfm.201301048

$$V_{OC}(I, T) \approx V_0 + n\frac{k_B T}{e} \ln \frac{I}{I_0} \quad (1)$$

where $eV_0 = E_g$ is the band gap in the case of an inorganic semiconductor (organic semiconductors will be discussed below), n is the diode ideality factor, and k_B the Boltzmann constant. I_0 is a constant with the unit of an intensity. It depends on the band gap and the densities of state (DOS) in the valence and conduction band. The approximation in Equation (1) is valid for $I << I_0 \exp(-E_g(k_B T)^{-1})$.

For organic solar cells, the validity of Equation (1) has been derived for several levels of detail: I_0 can be identified with the recombination dynamics at the donor-acceptor interface, where V_0 is directly related to the effective gap, i.e., the energetic difference between the lowest unoccupied molecular orbital (LUMO) of the acceptor material and the highest occupied molecular orbital (HOMO) of the donor material.[27–30] Vandewal et al. derived eV_0 as the energy of the charge-transfer state E_{CT} at the donor-acceptor interface, and I_0 as a term which is proportional to the squared electronic coupling of donor and acceptor and the inverse quantum efficiency of the radiative charge-transfer recombination.[17] Rand et al. have previously identified eV_0 experimentally with the effective donor-acceptor-gap E_g^{eff} (i.e., the energetic distance between the electron affinity (EA) of the acceptor and the ionization potential (IP) of the donor) less a constant value accounting for Coulomb interaction.[31] Nelson et al. derived a relation which is compatible with Equation (1) from a generation-recombination approach, identifying eV_0 with the energy gap and I_0 with a recombination coefficient proportional to the oscillator strength of a sensitizer.[32] In a similar approach, related to donor-acceptor based devices, eV_0 was identified with the effective HOMO-LUMO gap reduced at low T by an additional term proportional to the width of the energetic distribution of the DOS.[33] The value of the ideality factor n is usually between 1 and 2. It can be identified with the prevailing recombination mechanism.[34] The validity of the linear $V_{OC}(T)$ behavior is reported to be limited to moderate temperatures (i.e., typically not below 200 K), however showing a strong dependence on the specific material system under investigation, as initially shown for experimental data,[35,36] and more recently modeled by an interpretation based on generation-recombination calculations[33] and energetic barriers at the contacts.[37] In the discussion of the effective gap, the IP and EA are sometimes used ambiguously with HOMO and LUMO energies in thin films. In this work, we refer to IP and EA, because these quantities are experimentally accessible in thin films as the onset in ultraviolet photoelectron spectroscopy (UPS) and inverse photoemission spectroscopy (IPES).

The quantitative correlation between E_g^{eff} and V_{OC} is a matter of debate. It is further complicated by the inaccuracies of the energy level definitions and measurements, particularly of the EA in thin films. We show that the linear extrapolation $V_0 = V_{OC}(T \rightarrow 0\ K)$ is a well-defined device property of a bulk heterojunction organic solar cell with doped charge transport layers. We show that V_0 is independent of the used hole transport material, and that an influence of the mixing ratio of donor and acceptor cannot be detected. By varying the donor-acceptor material system, we show that E_g^{eff} can be quantitatively correlated to V_0 through identity.

3. Experimental Section

The organic solar cells investigated in this work are based on a bulk heterojunction of the two active materials – donor and acceptor – sandwiched between doped transport layers, according to the p-i-n concept.[5,38] Intrinsic layers of donor and acceptor can be introduced between the bulk heterojunction and the transport layers to improve light absorption and to avoid exciton separation between the hole (resp. electron) transport material and the acceptor (resp. donor).[39] The devices are fabricated on glass substrates which are coated with indium tin oxide (ITO; Thin Film Devices, Anaheim, CA, USA; 90 nm, 30 Ω/□) as transparent contact. The organic layers and the metal contact are deposited by thermal evaporation in vacuum (base pressure below 10^{-6} mbar). The layer thickness is controlled by quartz crystal micro balances. Doped layers and blend layers are fabricated by co-evaporation of two materials using separate thickness controls. The metal top contact is deposited by thermal evaporation through a shadow mask. The geometric overlap of metal and ITO contact defines the approximately square shaped active device area of 6.44 mm^2. The devices are encapsulated with a glass cavity glued on the substrate. A moisture getter[40] is placed inside the encapsulation to ensure long device lifetime.

The following materials are used (see Section 6 for chemical names, references, and details). As donor and/or hole transporting materials, α-NPD, BPAPF, CuPc, DCV-5T-Bu, Di-NPD, F4-ZnPc, MeO-TPD, P4-Ph4-DIP, Ph2-benz-Bodipy, and ZnPc are used. As acceptor and/or electron transporting materials, C_{60}, C_{70}, and BPhen are used. F6-TCNNQ and NDP9 are used as p-dopants, AOB and $W_2(hpp)_4$ as n-dopants.

The effective gap of a material system is calculated as $E_g^{eff} = IP^{donor} - EA^{acceptor}$. The IPs of the materials are determined by UPS in thin films. Experimental details are explained in ref. [41]. The experimental relative accuracy for the comparison of several measurements from the used tool is $\Delta IP_{rel} = 50$ meV. All UPS measurements might additionally be affected by a systematic offset of less than $\Delta IP_{abs} = 130$ meV. The EA of C_{60} is taken from ref. [42] as (4.0 ± 0.3) eV, a value that is in good agreement with more recent numbers.[43,44] The absolute uncertainties do not affect the resolution of the relation between energy levels, which is investigated in this work, because all E_g^{eff} values are calculated with the same EA value of C_{60} and with IP values measured at the same tool. The relevant accuracy is only subject to the much better relative resolution of the energy levels. The EA of C_{70} is 50 meV higher than the one of C_{60}, according to ref. [45] interpreted with ref. [46].

The organic solar cells are characterized in vacuum inside a cryostat. The device temperature is varied in the range between 180 K and 400 K. As some of the samples degrade at elevated T, those measurements are only evaluated up to the T where the device behavior is stable over time. The samples are illuminated with a halogen light bulb (50 W) from a distance of approx. 10 cm. Its illumination intensity I_1 produces a photocurrent in the devices which is equivalent to approx. 0.6–1.2 suns, depending on the materials used. In the intensity dependent measurements, the intensity is reduced down to approximately 0.2% of I_1. The exact absolute value of the illumination intensity is not required for the evaluation used

here, because the extrapolation to V_0 is independent of the illumination intensity. Heating effects from the illumination are compensated by a respective calibration of the setup to ensure a constant sample temperature at varying I. The absolute temperature resolution in the measurements is better than 5 K, the relative resolution between measurement points is better than 3 K.

The V_{OC} is measured with a source measure unit (Keithley 2400). It is interpolated from the two points of the current-voltage characteristic where the sign of the current density changes. The current-voltage characteristic is taken with a step-width of 50 mV. The accuracy is better than $\Delta V_{OC} \approx 30$ mV.

4. Results and Discussion

4.1. Determination of V_0

In the following section, the evaluation method for V_0 and its validity are discussed. It is demonstrated with the T and I dependent current-voltage characteristic of a device, which is based on a ZnPc:C_{60} bulk heterojunction: ITO/p-ZnPc (9 wt% F6-TCNNQ; 17 nm)/ZnPc:C_{60} (1:2.2 volume ratio; 37 nm)/C_{60} (19 nm)/n-C_{60} (2 wt% W_2(hpp)$_4$; 19 nm)/Al (100 nm).

From the measured j-V curves (**Figure 1**), $V_{OC}(T)$ can be extracted. This measurement is performed with varying I and the resulting data (**Figure 2**) is analyzed according to Equation (1). The T dependence of V_{OC} is linear with negative slope while the I dependence of V_{OC} is logarithmic. Both can be simultaneously fitted with one set of parameters, because V_0 is a T and I independent property of the device. The resulting values are $V_0 = 1.04$ V with a standard deviation of 6 mV, $I_0 = 5 \times 10^7 I_1$, and $n = 1.13$. This confirms that if $V_{OC}(T)$ is linear, V_0 can be obtained consistently with Equation (1) by extrapolating $V_{OC}(T)$ to 0 K. The value of $V_0 = 1.04$ V is in good agreement with the effective gap $E_g^{eff} = IP^{ZnPc} - EA^{C60} = (5.07 - 4.0)$ eV = 1.07 eV. The uncertainties of this E_g^{eff} determination will be discussed below. The uncertainties of V_0 from this measurement sum up to an experimental accuracy of $\Delta_{exp} V_0 \approx 50$ mV. For the overall accuracy ΔV_0, the standard deviation of the fit, has to be added: It is 6 mV for the measurement above and is determined separately for the further measurements.

4.2. Hole Transport Material Variation

The influence of the hole transport material (HTM) on V_0 is investigated in a series of solar cells based on a ZnPc:C_{60} bulk heterojunction, where the HTM is varied. The device stack is ITO/p-HTM (10 nm)/ZnPc (25 nm)/ZnPc:C_{60}(1:1, 10 nm)/C_{60} (50 nm)/n-C_{60} (5 wt% AOB; 10 nm)/Al (100 nm). The following materials are used as HTMs: ZnPc, MeO-TPD, α-NPD, and BPAPF. BPAPF is p-doped with 5 wt% NDP9, the other HTMs are p-doped with 5 wt% F6-TCNNQ. According to the IPs of the HTMs (**Table 1**), extraction barriers are expected in the devices with α-NPD and BPAPF, because their IPs are larger than the IP of ZnPc.[16]

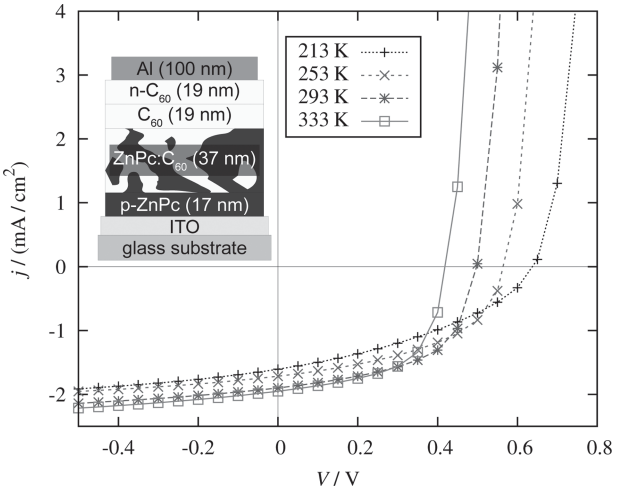

Figure 1. T dependent j-V characteristics of a ZnPc:C_{60} bulk heterojunction solar cell. Lines are connections between measurement points (symbols). Inset: stack sequence of the device (details given in the text).

From T dependent V_{OC} measurements, V_0 is constant in all devices (Table 1). Its value does not change within the measurement accuracy. We conclude that V_0 is not influenced by a doped HTM with a similar or higher IP than the donor, although other solar cell parameters like fill factor and efficiency vary a lot.[16] This can be understood assuming a good Ohmic contact between the ITO and the doped HTL.[47] It results in a common Fermi level in the HTL and contact, which is equal to the quasi-Fermi level of holes in the donor. The extraction barriers do not have an effect here because no current is flowing at V_{OC}. An injection barrier is avoided, because in that case we expect an additional reduction of V_{OC} due to increased recombination at the interface,[16] rendering the V_0 extrapolation invalid.

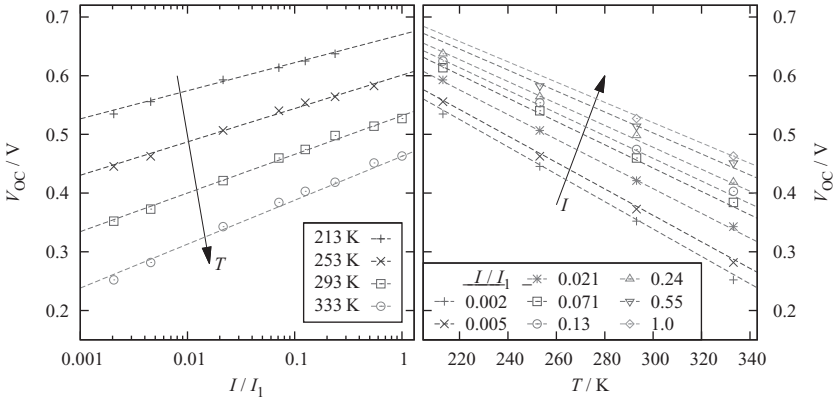

Figure 2. $V_{OC}(I,T)$ of the ZnPc:C_{60} solar cell shown in Figure 1 (same data plotted twice; at low temperatures, the highest illumination intensities have not been measured). All measured data points are simultaneously fitted (lines) by Equation (1) with a single set of parameters, where $V_0 = 1.04$ V with a standard deviation of 6 mV, $I_0 = 5 \times 10^7 I_1$, and $n = 1.13$ are the resulting values.

Table 1. V_0 of ZnPc:C_{60} solar cells with different HTMs and the *IP*s of the HTMs. The error given is the standard deviation for V_0 from the linear fit of $V_{OC}(T)$, the experimental accuracy is $\Delta_{exp}V_0 \approx 50$ mV.

HTM	*IP* [eV]	V_0 [V]
MeO-TPD	5.05	1.10 ± 0.019
ZnPc	5.07	1.08 ± 0.012
α-NPD	5.4	1.10 ± 0.013
BPAPF	5.6	1.08 ± 0.018

4.3. Donor:Acceptor Stoichiometry Variation

The influence of the donor:acceptor stoichiometry on V_0 is investigated with a separate set of samples. At room temperature, V_{OC} is influenced by the mixing ratio of donor and acceptor. In polymer solar cells, V_{OC} is reported to decrease with increasing Fullerene content.[48] In the case of ZnPc:C_{60}, it increases for high C_{60} concentration,[49] while in the similar material system CuPc:C_{60} the effective gap is reported to stay constant.[50] At very high Fullerene content, V_{OC} is independent of the HOMO of the donor for both polymers and small molecules.[51,52] We determine V_0 in a series of solar cells varying the ZnPc:C_{60} stoichiometry between approx. 4:1 and 1:7 while keeping the other layers unchanged. The device structure is ITO/ p-Di-NPD (5 wt% NDP9; 60 nm)/ZnPc:C_{60} (27 nm)/C_{60} (38 nm)/BPhen (6 nm)/Al (100 nm). The *IP* of Di-NPD is 5.3 eV, i.e., it is a suitable HTM for ZnPc as donor (see above). The thin BPhen layer at the metal contact is known to result in a good electronic contact to C_{60}.[53] In all devices, the value of V_0 (see **Figure 3**) is constant within ± 35 mV, which is less than the experimental error $\Delta_{exp}V_0$ = 50 mV. Averaging over all V_0 measurement points results in V_0^{avr} = (1.07 ± 0.02) V (standard deviation). From these measurements, we do not find a systematic dependence of V_0 on the mixing ratio. Consequently, V_0 is a property of the material combination and independent of the mixing ratio of the heterojunction.

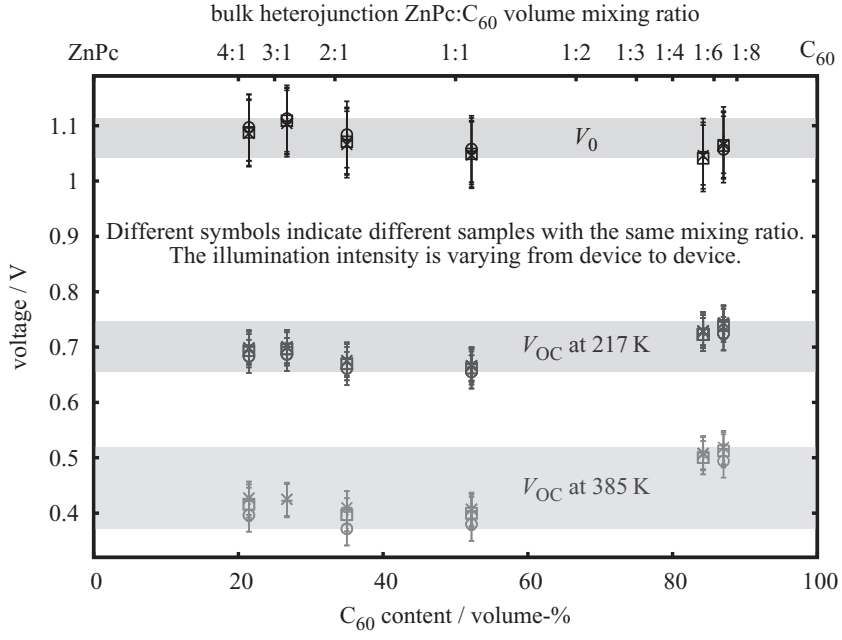

Figure 3. V_{OC} measured at 217 K and at 385 K, and extrapolated V_0 for different mixing ratios of the ZnPc:C_{60} bulk heterojunction. Each value for V_0 is extrapolated from a series of measurement points between 217 K and 385 K. V_0 fluctuates by ±35 mV. The error bars for V_0 include the statistical error of the extrapolation.

4.4. Donor:Acceptor Material Variation

The influence of E_g^{eff} on V_0 is investigated in a series of solar cells with different donor and acceptor materials. We use CuPc, MeO-TPD, ZnPc, P4-Ph4-DIP, Ph2-benz-Bodipy, α-NPD, DCV-5T-Bu, F4-ZnPc, and BPAPF as donors. They represent a broad variety of families of molecules used in small molecular organic solar cells. All donors are combined with C_{60} as acceptor. Additionally, C_{70} is used as acceptor in a sample with ZnPc as donor. The complete layer structures of all devices are listed in the supporting information. For most of the investigated material combinations, stacks and illumination intensities are found where V_0 can be determined reliably.

In **Figure 4**, the values of V_0 are related to the corresponding values of E_g^{eff}. The E_g^{eff} values are calculated with respect to the value EA^{C60} = 4.0 eV. The two quantities eV_0 and E_g^{eff} coincide for most material systems within the measurement accuracy. With F4-ZnPc:C_{60}, two different geometries are measured, a "p-i-n" sample, as well as two "n-i-p" samples where the transparent contact is the cathode. V_0 in the "n-i-p" devices is reduced by approx. 50 meV compared to the "p-i-n" device, which is within the resolution of the experimental data.

In the devices based on the material systems α-NPD:C_{60} and BPAPF:C_{60}, the slope of $V_{OC}(T)$ is not constant, but decreases for lower T, which might be related to the energy distribution of the electronic states,[33] a transition to another regime of recombination dynamics,[54] or a saturation effect in devices with non-Ohmic contacts.[37] The latter is less probable, since all other devices with doped organic layers as contact materials do not show this behavior. For α-NPD:C_{60} the reduced range T = 340–385 K is fitted. For BPAPF:C_{60} a linear fit is not possible. It was tried to be fitted with the model from Garcia-Belmonte et al.,[33] attributing the low T behavior to the energetic disorder of the frontier orbitals.[55] However, the fit results scatter largely among nominally identical devices and at this stage we cannot obtain reliable data for this approach. This material system is hence not regarded in the further evaluation.

The relation between V_0 and E_g^{eff} is compatible with a linear approximation with slope 1. This is shown with an accuracy of 50 meV for E_g^{eff} and (50–70) meV for V_0. In the presented measurements, an offset between eV_0 and E_g^{eff} is not found. This might be coincidence, due to the possible systematic error of the E_g^{eff} determination (see Section 3). A possible

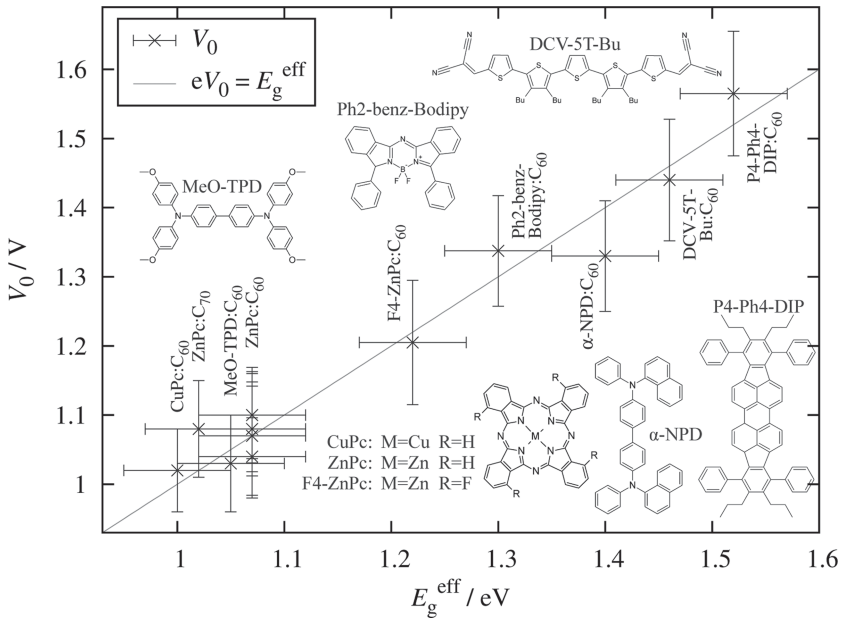

Figure 4. Extrapolated V_0 of several donor:acceptor material systems related to their effective gaps $E_g^{eff} = EA^{acceptor} - IP^{donor}$. All measurement points are within the experimental error from the identity relation $eV_0 = E_g^{eff}$ (line). The molecular structures of the donor materials are shown as insets. The error bars of E_g^{eff} reflect the accuracy of the *IP* determination via UPS.

offset could be expressed through an offset energy $eV_0 = E_g^{eff} + E_{offset}$ which is independent of the material system under investigation, shifting all measurement points in Figure 4 into the same direction. This means that the quantitative comparison of different effective gaps is still possible with an accuracy of ≈100 meV or better, no matter whether E_{offset} is present or not. The origin of E_{offset} might be the sum of several effects. For polymer based organic solar cells, Vandewal et al. showed that V_0 can be related to the energy of the charge-transfer complex at the donor-acceptor interface.[17] If this would be applicable to the devices investigated in this work, it would identify $-E_{offset}$ with the charge-transfer binding energy, but it seems unlikely that this value would be material independent. Another possible contribution might be the difference between the transport levels and the frontier orbital energies in disordered semiconductors, leading to the question about how the *EA* and *IP* values are obtained from the spectra and, consequently, how exactly the effective gap is defined. Since recent IPES measurements[43,44] indicate approx. the same *EA* values as used in this work, but with better accuracy, the actual uncertainty might be lower than assumed here. These values, confirmed by higher accuracy measurements,[44,56] suggest that E_{offset} is actually zero with respect to all achieved accuracy.

From the $V_{OC}(I,T)$ characteristics, it can be concluded that $eV_0 = E_g^{eff}$ is within the experimental error, independent of the material system. It seems that eV_0 plays the same role for V_{OC} in organic bulk heterojunction solar cells as does the band gap E_g between the valence band and the conduction band in inorganic solar cells.

The measurements include a broad variety of materials in the heterojunction and they include devices with variations in the stack design. These variations do not have an influence on V_0 within the achieved accuracy if the following requirements are fulfilled: The device must be based on a bulk heterojunction consisting of donor and acceptor, or a hybrid bulk-flat heterojunction where a bulk heterojunction is sandwiched between donor and acceptor. Flat heterojunction devices do not always follow Equation (1), because the extrapolation of $V_{OC}(T)$ to 0 K can be different for varying *I*.[57] Ohmic contacts are required between the organic layers and the contacting layers (metal, ITO).[37] These are realized with doped organic transport layers. Injection barriers between a transport layer and the respective heterojunction material[58] should be avoided, because they can lead to a reduced open-circuit voltage, which is not a sole property of the heterojunction, but strongly influenced by the respective transport layer.[16]

4.5. V_{OC} at Room Temperature

The comparison of V_{OC} at room temperature can in specific cases give some information about the effective gap.[20,30] The relation is applicable e.g. if the materials under observation have very similar properties. For many materials, the trend of V_{OC} at room temperature agrees qualitatively with E_g^{eff}, but this is not always reliable.[22] Differences have been illustrated experimentally by comparing tetracene and rubrene[21] and can be related to the energetic disorder at the donor-acceptor interface and the reorganization energy.[55] To give another example, the ZnPc:C_{60} samples from the HTM variation (see above) are compared to 4 structures with the same layer sequence except that MeO-TPD is used as donor instead of ZnPc. Several samples of all 8 structures are measured at room temperature with a sun simulator at a constant intensity of ≈1 sun. The V_{OC} of the ZnPc:C_{60} devices is in the range of (0.45–0.48) V, while in the MeO-TPD:C_{60} devices all V_{OC} values are in the range of (0.57–0.58) V. This is a difference of at least 100 meV, although E_g^{eff} is expected to be approximately the same in both material systems and ZnPc shows stronger light absorption. In contrast, V_0 is similar for both material systems (see above), and compatible with the E_g^{eff} values. The comparison between V_{OC} at room temperature and the effective gap of the other investigated materials is shown in **Figure 5**. There, an opposite trend can also be observed when comparing e.g., P4-Ph4-DIP:C_{60} with DCV-5T-Bu:C_{60} or α-NPD:C_{60} with Ph2-benz-Bodipy:C_{60}.

The reason for this deviation is that at room temperature, V_{OC} is lower than the effective donor-acceptor-gap, and the value of this reduction (i.e., implicitly I_0) depends on the specific device properties and material system used.[23] It can be related to the energetic distribution of the hole transport level of the donor and the electron transport level of the acceptor, according to ref. [55], where the offset between the effective gap and V_{OC} at room temperature is calculated to approx. 500 meV upon an energetic disorder of $\sigma = 100$ meV. From the observed

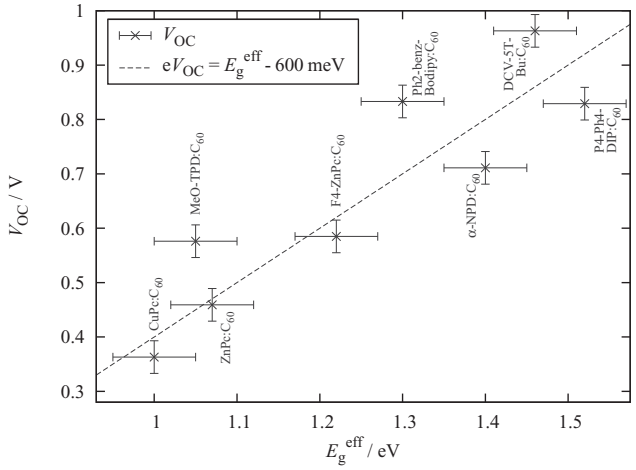

Figure 5. V_{OC} at room temperature of several solar cells with different donor materials related to their effective gaps. The difference is ≈600 meV in average, as depicted by the dashed line. However, deviations from this linear dependence are beyond the experimental errors for several material systems. A reliable linear relation at room temperature can consequently not be observed.

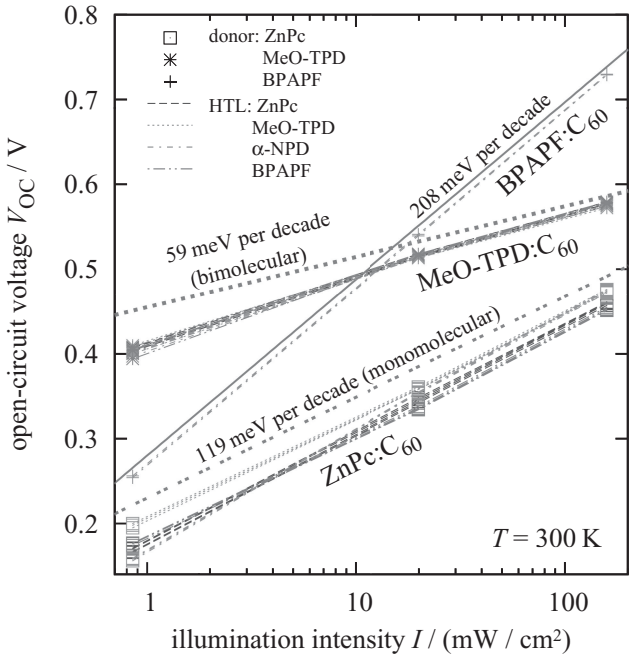

Figure 6. V_{OC} at room temperature as a function of illumination intensity I of several solar cells with different donor materials (indicated by point styles) and hole transport materials (indicated by line styles). The expected slope for bimolecular recombination and for monomolecular recombination is plotted as dotted lines as a guide to the eye for the ZnPc:C_{60} devices and for the MeO-TPD:C_{60} devices, respectively, and a slope of 208 meV per decade is shown for comparison to the BPAPF:C_{60} devices. For every structure, several nominally identical devices were measured. For ZnPc:C_{60} and MeO-TPD:C_{60}, all four HTLs yield reproducible data. Especially for MeO-TPD:C_{60}, the data points lie very close. For BPAPF:C_{60}, only the combination with α-NPD as HTL yield reproducible results and the respective data points are shown here.

offsets between V_0 and V_{OC} at room temperature, which are in the range of (450–700) meV in our material systems, it can be concluded that the energetic disorder of the transport levels is approximately ≥100 meV. The stoichiometry variation discussed in Section 4.3 furthermore leads to the conclusion that the energetic disorder is largest in a balanced mixing ratio (1:1 or 2:1), while the energetic distribution gets narrower for increasing C_{60} content.

In summary, at the current state of research it is virtually not possible to effectively determine I_0 from a microscopic approach. The temperature and illumination dependent voltage measurements, however, are a macroscopic experimental approach which is capable to resolve this issue. For the mathematical determination of V_0, the measurement of either $V_{OC}(I)$ or $V_{OC}(T)$ would be sufficient. However, to confirm the physical validity of the extrapolation, the illumination and temperature dependent characterization $V_{OC}(I,T)$ is required.

4.6. Recombination

From the data of the discussed devices, some more details about the dominating recombination mechanisms at V_{OC} can be derived regarding the intensity dependence of the open-circuit voltage $V_{OC}(I)$. The slope in a semi-logarithmic plot is shown in **Figure 6** at room temperature. It yields information about whether direct bimolecular recombination or monomolecular (e.g., trap-assisted) recombination is dominating.[28,54] A slope of $S_0 = k_B T e^{-1} \ln(10)$ per decade (≈59 meV per decade at room temperature) indicates bimolecular recombination, and $2S_0 \approx$ 119 meV per decade indicates monomolecular recombination. The devices with a ZnPc:C_{60} bulk heterojunction clearly show monomolecular behavior, indicating that recombination is dominated by trapped charges, either in extrinsic traps (e.g., degraded molecules) or in deep states of the energetically distributed frontier orbitals of donor or acceptor. This finding is independent of the used HTM with only negligible deviations. The devices with a MeO-TPD:C_{60} heterojunction show a transition from monomolecular to bimolecular recombination, which is reported elsewhere in detail for this material system.[54] Also in this case, the result is valid for all used HTMs. In contrast, the BPAPF:C_{60} heterojunction shows a much higher slope of approx. 208 meV ≈ $3.5S_0$ per decade. This value is observed for α-NPD as HTM. The high slope can be attributed to an elevated ideality factor and might indicate additional trap states for recombination.[59]

5. Conclusion and Outlook

A linear $V_{OC}(T)$ dependence, as commonly found in photovoltaic devices, is observed in a number of bulk heterojunction organic solar cells based on different donor:acceptor material combinations. We have shown that in these devices the extrapolation of V_{OC} to 0 K, denoted as V_0, is a quantity which is independent of the illumination intensity and directly related to the effective donor-acceptor-gap E_g^{eff} of the bulk heterojunction within experimental error. This confirms that E_g^{eff} is the

quantity which is analogous to the band gap in inorganic solar cells with respect to V_{OC}. We have shown that the reliability of such V_0 determination can be verified and essentially improved by varying parameters like the illumination intensity or the transport layer materials and checking that V_0 stays constant.

These findings allow for the direct determination of E_g^{eff} values through determination of V_0, and comparison of different photoactive bulk heterojunctions. This approach opens a pathway to determining the *IP* or *EA* of a material. The values are essential for a quantitative understanding of the energetic structure of organic electronic devices and especially the open-circuit voltage of organic solar cells.

6. Materials

The following materials are used as donor and/or hole transporting materials (see Figure 4 for molecular structures): N,N′-di(naphthalen-1-yl)-N,N′-diphenyl-benzidine (α-NPD; Sensient, Milwaukee, WI, USA; density used for thickness calculation: 1.14 g cm^{-3}), 9,9-bis[4-(N,N-bis-biphenyl-4-yl-amino)phenyl]-9H-fluorene (BPAPF; Lumtec, Hsin-Chu, Taiwan; 1.2 g cm^{-3}), copper-phthalocyanine (CuPc; ABCR, Karlsruhe, Germany; 1.3 g cm^{-3}), 3′,3‴,4′,4‴-tetrabutyl-bis-dicyanovinyl-α-quinquethiophene (DCV-5T-Bu; see ref.[60]; University of Ulm, Germany; 1.3 g cm^{-3}), N,N′-diphenyl-N,N′-bis(4′-(N,N-bis(naphth-1-yl)-amino)-biphenyl-4-yl)-benzidine (Di-NPD; Sensient; 1.14 g cm^{-3}), tetrafluoro-zinc-phthalocyanine (F4-ZnPc; BASF, Ludwigshafen, Germany; see ref.[61,62]; 1.3 g cm^{-3}), N,N,N′,N′-tetrakis(4-methoxyphenyl)-benzidine (MeO-TPD; Sensient; 1.46 g cm^{-3}), 2,3,10,11-tetrapropyl-1,4,9,12-tetraphenyl-diindeno[1,2,3-cd:1′,2′,3′-lm] perylene (P4-Ph4-DIP; see ref.[63]; 1.04 g cm^{-3}), Ph2-benz-Bodipy (see ref.[64]; 1.1 g cm^{-3}), and zinc-phthalocyanine (ZnPc; ABCR; 1.55 g cm^{-3}). The following materials are used as acceptor and/or electron transporting material: the Fullerenes C_{60} (CreaPhys, Dresden, Germany; 1.63 g cm^{-3}) and C_{70} (BuckyUSA, Houston, TX, USA; 1.54 g cm^{-3}), and bathophenanthroline (BPhen; Lumtec; 1.24 g cm^{-3}). The materials used as p-dopants are 2,2-(perfluoronaphthalene-2,6-diylidene) (F6-TCNNQ; see ref.[65,66]) and NDP9 (Novaled, Dresden, Germany). The materials used as n-dopants are acridine orange base (AOB; Sigma Aldrich, Steinheim, Germany) and tetrakis(1,3,4,6,7,8-hexahydro-2H-pyrimido[1,2-a]pyrimidinato)ditungsten (II) ($W_2(hpp)_4$; see ref.[67,68]; Novaled). C_{60}, DCV-5T-Bu, F4-ZnPc, F6-TCNNQ, NDP9, and $W_2(hpp)_4$ are used as received, all other materials are purified by vacuum sublimation prior to device fabrication.

Supporting Information

Supporting Information is available from the Wiley Online Library or from the author.

Acknowledgements

The work was supported by the German Federal Ministry of Education and Research (BMBF) in the framework of the Projects No. 13N9720 (project "OPEG") and 13N10142 ("Multifunktionale Speichersysteme"), and the Heinrich Böll Foundation. The authors acknowledge Novaled AG, Germany, for providing dopants. The authors thank Prof. Bäuerle from the University of Ulm for supplying DCV-5T-Bu, BASF for supplying F4-ZnPc, Hannah Ziehlke and Steffen Pfützner for contributing samples, and Selina Olthof for UPS measurement data.

Received: March 26, 2013
Published online: June 19, 2013

[1] Heliatek, www.heliatek.com, (accessed May 2013).
[2] M. A. Green, K. Emery, Y. Hishikawa, W. Warta, E. D. Dunlop, *Prog. Photovoltaics* **2013**, *21*, 1.
[3] C. Tang, *Appl. Phys. Lett.* **1986**, *48*, 183.
[4] M. Hiramoto, H. Fujiwara, M. Yokoyama, *Appl. Phys. Lett.* **1991**, *58*, 1062.
[5] B. Maennig, D. Gebeyehu, P. Simon, F. Kozlowski, A. Werner, F. Li, S. Grundmann, S. Sonntag, M. Koch, K. Leo, M. Pfeiffer, H. Hoppe, D. Meissner, N. S. Sariciftci, I. Riedel, V. Dyakonov, J. Parisi, J. Drechsel, *Appl. Phys. A* **2004**, *79*, 1.
[6] M. Pfeiffer, T. Fritz, J. Blochwitz, A. Nollau, B. Plönnings, A. Beyer, K. Leo, in *Advances in Solid State Physics* (Ed: B. Kramer), Vieweg, Braunschweig **1999**; pp. 77–90.
[7] K. Suemori, T. Miyata, M. Hiramoto, M. Yokoyama, *Jpn. J. Appl. Phys.* **2004**, *43*, L1014.
[8] M. Riede, C. Uhrich, R. Timmreck, J. Widmer, D. Wynands, M. Levichkova, M. Furno, G. Schwartz, W. Gnehr, M. Pfeiffer, K. Leo, in *2010 35th IEEE Photovoltaic Specialists Conference,*IEEE, **2010**, p. 513.
[9] M. Hiramoto, M. Suezaki, M. Yokoyama, *Chem. Lett.* **1990**, *19*, 327.
[10] J. Drechsel, B. Männig, F. Kozlowski, M. Pfeiffer, K. Leo, H. Hoppe, *Appl. Phys. Lett.* **2005**, *86*, 244102.
[11] M. Riede, C. Uhrich, J. Widmer, R. Timmreck, D. Wynands, G. Schwartz, W.-M. Gnehr, D. Hildebrandt, A. Weiss, J. Hwang, S. Sudharka, P. Erk, M. Pfeiffer, K. Leo, S. Sundarraj, *Adv. Funct. Mater.* **2011**, *21*, 3019.
[12] M. C. Scharber, D. Mühlbacher, M. Koppe, P. Denk, C. Waldauf, A. J. Heeger, C. J. Brabec, *Adv. Mater.* **2006**, *18*, 789.
[13] M. Gruber, J. Wagner, K. Klein, U. Hörmann, A. Opitz, M. Stutzmann, W. Brütting, *Adv. Energy Mater.* **2012**, *2*, 1100.
[14] O. V. Mikhnenko, F. Cordella, A. B. Sieval, J. C. Hummelen, P. W. M. Blom, M. A. Loi, *J. Phys. Chem. B* **2008**, *112*, 11601.
[15] M. Schober, M. Anderson, M. Thomschke, J. Widmer, M. Furno, R. Scholz, B. Lüssem, K. Leo, *Phys. Rev. B* **2011**, *84*, 165326.
[16] W. Tress, K. Leo, M. Riede, *Adv. Funct. Mater.* **2011**, *21*, 2140.
[17] K. Vandewal, K. Tvingstedt, A. Gadisa, O. Inganäs, J. V. Manca, *Phys. Rev. B* **2010**, *81*, 1.
[18] A. E. Jailaubekov, A. P. Willard, J. R. Tritsch, W.-L. Chan, N. Sai, R. Gearba, L. G. Kaake, K. J. Williams, K. Leung, P. J. Rossky, X.-Y. Zhu, *Nat. Mater.* **2012**, *12*, 66.
[19] C. Uhrich, D. Wynands, S. Olthof, M. Riede, K. Leo, S. Sonntag, B. Maennig, M. Pfeiffer, *J. Appl. Phys.* **2008**, *104*, 043107.
[20] C. J. Brabec, A. Cravino, D. Meissner, N. S. Sariciftci, T. Fromherz, M. T. Rispens, L. Sanchez, J. C. Hummelen, *Adv. Funct. Mater.* **2001**, *11*, 374.
[21] M. D. Perez, C. Borek, S. R. Forrest, M. E. Thompson, *J. Am. Chem. Soc.* **2009**, *131*, 9281.
[22] A. Maurano, R. Hamilton, C. G. Shuttle, A. M. Ballantyne, J. Nelson, B. O'Regan, W. Zhang, I. McCulloch, H. Azimi, M. Morana, C. J. Brabec, J. R. Durrant, *Adv. Mater.* **2010**, *22*, 4987.
[23] D. Credgington, R. Hamilton, P. Atienzar, J. Nelson, J. R. Durrant, *Adv. Funct. Mater.* **2011**, *21*, 2744.
[24] P. Würfel, *Physik der Solarzellen*; 2. Auflage.; Spektrum Akademischer Verlag, Heidelberg **2000**.
[25] P. Würfel, *Chimia* **2007**, *61*, 770.
[26] J. Bisquert, G. Garcia-Belmonte, *J. Phys. Chem. Lett.* **2011**, *2*, 1950.
[27] L. J. A. Koster, V. D. Mihailetchi, R. Ramaker, P. W. M. Blom, *Appl. Phys. Lett.* **2005**, *86*, 123509.
[28] S. R. Cowan, A. Roy, A. J. Heeger, *Phys. Rev. B* **2010**, *82*, 245207.
[29] A. K. Thakur, G. Wantz, G. Garcia-Belmonte, J. Bisquert, L. Hirsch, *Sol. Energy Mater. Sol. Cells* **2011**, *95*, 2131.
[30] S. Yamamoto, A. Orimo, H. Ohkita, H. Benten, S. Ito, *Adv. Energy Mater.* **2012**, *2*, 229.
[31] B. Rand, D. Burk, S. Forrest, *Phys. Rev. B* **2007**, *75*, 115327.
[32] J. Nelson, J. Kirkpatrick, P. Ravirajan, *Phys. Rev. B* **2004**, *69*, 035337.

[33] G. Garcia-Belmonte, *Sol. Energy Mater. Sol. Cells* **2010**, *94*, 2166.
[34] D. Cheyns, J. Poortmans, P. Heremans, C. Deibel, S. Verlaak, B. Rand, J. Genoe, *Phys. Rev. B* **2008**, *77*, 165332.
[35] I. Riedel, J. Parisi, V. Dyakonov, L. Lutsen, D. Vanderzande, J. C. Hummelen, *Adv. Funct. Mater.* **2004**, *14*, 38.
[36] V. Dyakonov, *Appl. Phys. A* **2004**, *79*, 21.
[37] D. Rauh, A. Wagenpfahl, C. Deibel, V. Dyakonov, *Appl. Phys. Lett.* **2011**, *98*, 133301.
[38] K. Walzer, B. Maennig, M. Pfeiffer, K. Leo, *Chem. Rev.* **2007**, *107*, 1233.
[39] D. Wynands, B. Männig, M. Riede, K. Leo, E. Brier, E. Reinold, P. Bäuerle, *J. Appl. Phys.* **2009**, *106*, 054509.
[40] From Dynic Ltd., Hong Kong
[41] S. Olthof, W. Tress, R. Meerheim, B. Lüssem, K. Leo, *J. Appl. Phys.* **2009**, *106*, 103711.
[42] W. Zhao, A. Kahn, *J. Appl. Phys.* **2009**, *105*, 123711.
[43] A. Wilke, J. Endres, U. Hörmann, J. Niederhausen, R. Schlesinger, J. Frisch, P. Amsalem, J. Wagner, M. Gruber, A. Opitz, A. Vollmer, W. Brütting, A. Kahn, N. Koch, *Appl. Phys. Lett.* **2012**, *101*, 233301.
[44] H. Yoshida, *MRS Proc.* **2013**, *1493*, h04-03.
[45] Y. Yang, F. Arias, L. Echegoyen, L. P. F. Chibante, S. Flanagan, A. Robertson, L. J. Wilson, *J. Am. Chem. Soc.* **1995**, *117*, 7801.
[46] P. I. Djurovich, E. I. Mayo, S. R. Forrest, M. E. Thompson, *Org. Electron.* **2009**, *10*, 515.
[47] J. Blochwitz, *Org. Electron.* **2001**, *2*, 97.
[48] F. Piersimoni, S. Chambon, K. Vandewal, R. Mens, T. Boonen, A. Gadisa, M. Izquierdo, S. Filippone, B. Ruttens, J. D'Haen, N. Martin, L. Lutsen, D. Vanderzande, P. Adriaensens, J. V. Manca, *J. Phys. Chem. C* **2011**, *115*, 10873.
[49] M. Tietze, private communication **2013**.
[50] A. Opitz, M. Bronner, W. Brütting, M. Himmerlich, J. A. Schaefer, S. Krischok, *Appl. Phys. Lett.* **2007**, *90*, 212112.
[51] M. Zhang, H. Wang, H. Tian, Y. Geng, C. W. Tang, *Adv. Mater.* **2011**, *23*, 4960.
[52] B. Yang, F. Guo, Y. Yuan, Z. Xiao, Y. Lu, Q. Dong, J. Huang, *Adv. Mater.* **2013**, *25*, 572.
[53] P. Peumans, S. R. Forrest, *Appl. Phys. Lett.* **2001**, *79*, 126.
[54] W. Tress, K. Leo, M. Riede, *Appl. Phys. Lett.* **2013**, *102*, 163901.
[55] G. Garcia-Belmonte, J. Bisquert, *Appl. Phys. Lett.* **2010**, *96*, 113301.
[56] H. Yoshida, *Chem. Phys. Lett.* **2012**, *539-540*, 180.
[57] J. Widmer, K. Leo, M. Riede, *MRS Proc.* **2013**, *1493*, h06-01.
[58] J. Widmer, J. Fischer, W. Tress, K. Leo, M. Riede, unpublished.
[59] T. Kirchartz, B. E. Pieters, J. Kirkpatrick, U. Rau, J. Nelson, *Phys. Rev. B* **2011**, *83*, 115209.
[60] K. Schulze, C. Uhrich, R. Schüppel, K. Leo, M. Pfeiffer, E. Brier, E. Reinold, P. Bäuerle, *Adv. Mater.* **2006**, *18*, 2872.
[61] H. Brinkmann, C. Kelting, S. Makarov, O. Tsaryova, G. Schnurpfeil, D. Wöhrle, D. Schlettwein, *Phys. Status Solidi A* **2008**, *205*, 409.
[62] J. Meiss, A. Merten, M. Hein, C. Schuenemann, S. Schäfer, M. Tietze, C. Uhrich, M. Pfeiffer, K. Leo, M. Riede, *Adv. Funct. Mater.* **2012**, *22*, 405.
[63] J. Meiss, M. Hermenau, W. Tress, C. Schuenemann, F. Selzer, M. Hummert, J. Alex, G. Lackner, K. Leo, M. Riede, *Phys. Rev. B* **2011**, *83*, 165305.
[64] R. Gresser, M. Hummert, H. Hartmann, K. Leo, M. Riede, *Chem.–Eur. J.* **2011**, *17*, 2939.
[65] P. K. Koech, A. B. Padmaperuma, L. Wang, J. S. Swensen, E. Polikarpov, J. T. Darsell, J. E. Rainbolt, D. J. Gaspar, *Chem. Mater.* **2010**, *22*, 3926.
[66] H. Kleemann, C. Schuenemann, A. A. Zakhidov, M. Riede, B. Lüssem, K. Leo, *Org. Electron.* **2012**, *13*, 58.
[67] F. A. Cotton, N. E. Gruhn, J. Gu, P. Huang, D. L. Lichtenberger, C. A. Murillo, L. O. Van Dorn, C. C. Wilkinson, *Science* **2002**, *298*, 1971.
[68] T. Menke, D. Ray, J. Meiss, K. Leo, M. Riede, *Appl. Phys. Lett.* **2012**, *100*, 093304.